

Polymer Translocation through a Nanopore under a Pulling Force - A 3D Langevin Dynamics Simulation Study

Fikre Jida

Department of Physics, Bule Hora University, Ethiopia

ABSTRACT

Employing, the Langevin dynamics simulations study method, we investigate the dynamics of linear chain polymers' translocation into and out of a three-dimensional spherical cavity through a nanopore under a pulling force F . For the polymer translocations into the cavity, we observe different factors that influence on polymer translocation dynamics through a nanopore under a pulling force in Langevin dynamics simulations. Our focus on the influence of the chain length defined as $N = R_g/R$, R_g is the radius of gyration to the polymer and R is the cavity's radius, thermostat Langevin temperature T , the cavity pore size η and the pulling force F on the average translocation time. Thus, we obtain that the distribution of τ for the different chain lengths, it is symmetric and narrow for strong F . We also assure that $\tau \sim N^2$ and translocation velocity $v \sim N^{-1}$ for both moderate and strong F . Relatively for wide pore, three regimes are observed for τ as a function of F . τ is independent of F for weak F and lastly crosses over to $\tau \sim F^{-1}$ for strong force even for a moderate force. Finally, the waiting time, for monomer n and monomer $n+1$ to exit the pore, has a maximum for n close to the end of the chain, in contrast to the case where the polymer is driven by an external force within the pore. We also here present a computer simulation study of polymer translocation out of the cavity in a situation where the chain is initially confined to a closed spherical cavity in order to reduce the impact of conformational diversity on the translocation times. In particular, we investigate how the coefficient of variation of the distribution of translocation times can be minimized by optimizing both the volume and the aspect ratio of the cavity.

Keywords : Langevin Dynamics, ESPRESSO, translocation, coarse-grained, bead, linear polymer, scaling behavior, distribution of translocation time, thermostat Langevin.

I. INTRODUCTION

The transport of protein and nucleic acids through a nanometric pore size is crucial importance to life. *DNA* and *RNA* translocation across nuclear pore, protein transport through membrane channel and virus injection all these are basic notable examples to the main topic **Polymer Translocation**[1]. Moreover, it has a potential to revolutionary technological applications such as rapid DNA sequencing, protein

analysis filter of macromolecules sieves and control drug delivery are some applications of polymer translocation to technological revolutionary[2–5,7].b Due to wide range applications to revolutionary technology, recently Polymer translocation has become a popular research areas in polymer physics in which experimental [8, 9, 11, 13], simulation [14–16, 18, 20–30, 53].and theoretical studies[31,37–39, 55]. The dynamics of the translocation of polymer, since it can be depended on by so many factors, such

as the driving force in the nanopore, the sequence of the polymer and the geometry of the channel etc. and it, the polymer translocation is a complex and challenging problem. To understand the behavior of translocation recently a lot of researches have been done and reviewed on the study of the polymer translocation [40, 41, 43]. Polymer translocation involves a moment of polymer either into or out confined spaces. Recent, computer simulation theoretical studies in this area have mainly focused on the effect of different confine space, like as spherical or ellipsoidal cavities [45– 52, 54, 57, 59–63, 68]. Therefore, the Processes of polymer translocation into confined space is much more complex, compared with an unconfined space. Until now researchers have done a lot of work on the polymer translocation into unclosed confined space [13, 21]. A Langevin dynamics simulation study employs to investigate the dynamics of polymer translocation into space. Thus, in two dimensions a nonuniversal dependence relation observes that the average translocation time τ on the chain length N [21]. In the three dimensions, the confined space leads to non-universal dependence of average translocation time τ as a function of driving force F [21]. Inspired by the experiments [6, 15, 17], a number of recent theories [17, 32, 33, 35, 36, 53] have been developed for the dynamics of polymer translocation. Especially, the scaling of the translocation time τ with the chain length N is an important measure of the underlying dynamics and considered equilibrium entropy of the polymer as a function of the position of the polymer through the nanopore. Standard Kramer analysis of diffusion through this entropic barrier yields a scaling prediction of $\tau \sim N^2$ for the field-free translocation. For the forced translocation, a linear dependence of τ on N was suggested, which is in agreement with some experimental results[6, 15] for a α -hemolysin channel. However, as Chuang et al.[32] noted, the quadratic scaling behavior for the field-free translocation cannot be correct for a self-avoiding polymer. The reason is that the translocation time is

shorter than the equilibration time of a self-avoiding polymer, $\tau_{\text{equil}} \sim N^{1+2\nu}$, where ν is the Flory exponent [36]. According to scaling theory, they showed that for large N , translocation time scales approximately in the same manner as equilibration time. For the forced translocation, Kantor and Kardar [33] provided a lower bound for the translocation time that scales as $N^{1+\nu}$, by considering the unimpeded motion of the polymer. Most recently, investigations both free and forced translocation using both the two-dimensional fluctuating bond model with single-segment Monte Carlo moves [35, 36] and Langevin dynamic simulations [44, 53]. For the free translocation, it is numerically verified $\tau \sim N^{1+2\nu}$ by considering a polymer which is initially placed in the middle of the pore [35, 44]. For the forced translocation, it is found that a crossover scaling from $\tau \sim N^{2\nu}$ for relatively short polymers to $\tau \sim N^{1+\nu}$ for longer chains[36, 44]. In addition, it is also found that this crossover scaling remains unaffected for heteropolymer translocation [44]. Polymer translocation affects a large entropic barrier and thus most polymer translocation process requires a driving force, such as an external electric field used in the above-mentioned experiments. However, one can also investigate the use of other forces, such as a pulling force. With the development of manipulation of a single molecule, polymer motion can be controlled by optical tweezers [56]. This gives a motivation to study the translocation in which only the leading monomer experiences a pulling force. In addition, a new sequencing technique based on a combination of magnetic and optical tweezers for controlling the DNA motion has been reported [58]. Therefore it is of great significance to theoretically investigate the polymer translocation under a pulling force. Kantor and Kardar [33] have considered the scaling of τ with N and with the pulling force F . They have also tested the scaling behavior in a Monte Carlo simulation study of the fluctuation bond model. However, this model is only valid for moderate pulling forces. For strong pulling forces, the scaling of τ with N is different and needs to be

examined carefully. In addition, studies on translocation into confined geometries, in a space of characteristic size equal to its radius of gyration or lower and a very slit than its radius of gyration will shed light on the dynamics of the packaging of DNA inside virus capsid [64–66], where the entropic penalty is from both the limited volume and the additional self-exclusion of the chain. Many important details are still not clear, such as (a) the translocation probability, (b) the distribution of the translocation time, and (c) the average translocation time as a function of pulling force F , the chain length N , the cavity pore size and thermostat Langevin temperature T for the polymer translocation into confined geometry like spherical cavity the diagram is shown in the Fig.3. To this end, our aim in this paper, we investigate the dynamics of polymer translocation into and out of a 3D spherical nanocontainer using Langevin dynamics simulations study.

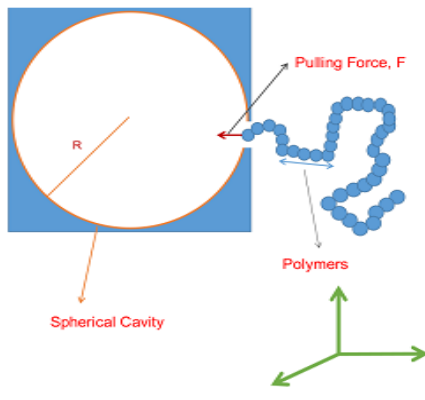


Figure 1: Schematic representation of polymer translocation through a pore into a 3D spherical compartment with radius R pulled by a force F in the cavity pore along the z axis (a) before translocation. The diameter of the pore is $D = 1.2\sigma$. and length $l = \sigma$.

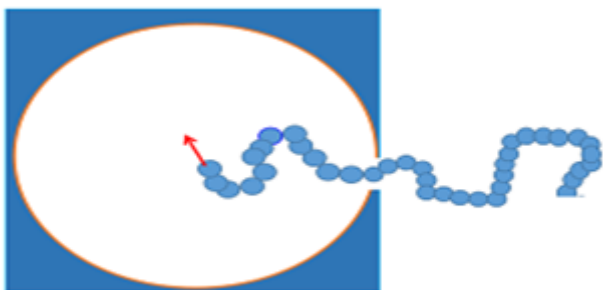


Figure 2: during translocation



Figure 3: after translocation

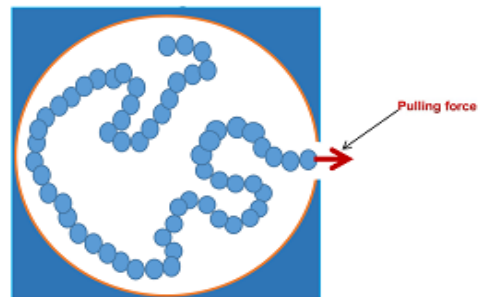


Figure 4: Schematic representation of the initial state ($t = 0$) for a polymer (with $N = 60$ monomers) inside a 3D spherical compartment with radius R pulled by a force F in the cavity pore along Z axis. The diameter of the pore is $D = 1.2\sigma$. and length $l = \sigma$.

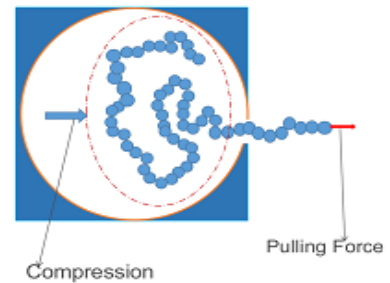


Figure 5: Schematic representation of polymer translocation through a pore out of a 3D spherical compartment with radius R pulled by a force F in the cavity pore along Z axis. The diameter of the pore is $D = 1.2\sigma$. and length $l = \sigma$.

II. METHODS AND MATERIAL

MODEL AND SIMULATIONS DETAILS

An insight of a perfect statistical analysis of the translocation time and its dependence on the polymer structure, nanopore size, and others, we have considered a coarse-grained model for the polymer walls of the cavity and the pore. Our aim is to define a model simple enough to

produce very extended ensembles of translocation events to completely characterize the statistical properties of the translocation time. In our numerical simulation study, we model the polymer chains as bead-spring chains of Lennard-Jones (LJ) particles with the Finite Extension Nonlinear Elastic (FENE) potential [69]. Excluded volume interactions between beads are modeled by a short-range repulsive LJ potential.

$$U_{LJ}(r) = \begin{cases} 4\varepsilon[(\frac{\sigma}{r})^{12} - (\frac{\sigma}{r})^6] + \varepsilon, & r \leq 2\frac{1}{2}\sigma \\ 0, & r > 2\frac{1}{2}\sigma \end{cases} \quad (1)$$

Where r is the distance between the two beads, σ is the diameter of a bead, and ε is the depth of the potential. The connectivity between neighboring monomers is modeled as a FENE spring (potential) with

$$U_{FENE}(r) = -\frac{1}{2}kR_0^2 \ln(1 - (\frac{r}{R_0})^2), \quad (2)$$

Where r is the distance between consecutive monomers, $k = 15\varepsilon/\sigma^2$ is the spring constant and $R_0 = 2\sigma$ is the maximum allowed separation between connected monomers. As shown in Fig. 1 and 4, we consider a three-dimensional (3D) geometry, the spherical cavity nanocontainer with a pore of width $D = 1.2\sigma$ and length $l = 1\sigma$ is formed by stationary wall particles within a distance σ from each other. Between all monomers wall particle pairs, there exists the same short-range repulsive LJ interaction as depicted above. Inside the pore, there exists a pulling force along the z -axis, as shown in Fig. 1 . Once the first monomer enters the pore, it will bear a repulsive force imposed by the inside wall of the pore and the polymer is pulled by the F to translocate along the z -axis into and out of a spherical geometry as shown in the Fig. 5. In Langevin dynamics simulation, each monomer is subjected to conservative, random and frictional forces, respectively.

$$m\ddot{r}_i = F_i^C + F_i^R + F_i^F, \quad (3)$$

Where m is the monomer's mass. The frictional force in the Langevin dynamics equation is formulated by

$$F_i^F = -\xi v_i \quad (4)$$

Where ξ is the friction coefficient, v_i is the bead's velocity. The conservative force in the Langevin dynamics equation consists of several terms.

$$F_i^C = -\nabla(U_{LJ} + U_{FENE}) \quad (5)$$

The pulling force is expressed as

$$F_{pulling} = F\hat{z} \quad (6)$$

Where F is the pulling force strength exerted exclusively on the monomer in the pore, and \hat{z} is a unit vector in which, the direction of the force corresponds to the nanopore-axis and towards the *Trans side*. And F_i^R is the random force satisfying the fluctuation-dissipation theorem. Polymer translocation is conducted under the influence of a constant nontime-dependent pulling force acting on the first monomer inside a nanopore so as to overcome a large entropic barrier during polymer translocation and to speed up the translocation process.

In this our work, we use the LJ parameters ε , σ , and m to fit the system energy, length and mass scales, respectively. As a result, their relationships among the parameters shown by in the following table.

Obsevable	Dimensions	LJ units	SI units
Length	L	σ	$1.0 \times 10^{-9} m$
Mass	M	m	$5.2 \times 10^{-25} kg$
Energy	E	ε	$4.1 \times 10^{-21} J$
Temperature	T	ε	295K
Force	E/L	ε/σ	4.1pN
Time	$\sqrt{ML^2/E}$	$\sqrt{m\sigma^2/\varepsilon}$	11.26ps
Friction	$\sqrt{EM/L^2}$	γ	$4.62 \times 10^{-14} kg/s$

Table 1: Main observables (with the appropriate dimensions) in Lennard Jones units, together with typically associated values in SI units for the real system. Note that $k_B=1$ in LJ units.

Initially, the first monomer of the chain is fixed at the cavity pore center then, the chain begins to relax on the cis side, as shown in Fig1 and 4. Once the total energy of the polymer chain fluctuates a little for a period of time, the polymer chain reaches equilibrium. The first monomer is released, at this moment set as time $t=0$, and start the translocation it is shown in Fig2 and 5. The chain may withdraw from nanopore and drift away under the influence of the entropy barrier. If the chain withdraws from the nanopore, the translocation process restarts. Once the last monomer enters or outs the trans side, the translocation process is over and the duration time is defined as translocation time τ , see Fig3 for translocation into the cavity. Thus the translocation time τ is defined as the time duration between the beginning of the translocation and the last bead/monomer of the chain entering into or out of the spherical cavity. Typically, the averaging is done over 1000 successful translocation events and the simulation is performed by employing free source code known as ESPRESSO which stands for an Extensible Simulation Package for Research on Soft Matter Systems.

III. RESULTS AND DISCUSSION

Into and out of the Cavity

The scaling behavior of for polymer in full three-dimensional confinement, such as a spherical cavity, is different compared with slit-like confinement and tube-like confinement. we first consider the equilibrium behavior of a linear chain of length N confined into a three-dimensional spherical nano container of the radius R , see Fig. 3. The translocations have been performed through a small pore by pulling one end of the polymer see Fig. 2 and 5. It is, the case of end polymer pulling while experimentally relevant [73] has been poorly considered by numerical simulations [33] until very recently [75]. Theory for biased polymer translocation aims at finding so-called critical

exponents ν and δ linking the mean translocation time to name the polymerization index and the bias force: $\tau \sim N \nu / F \delta$. As formerly discussed, many theories and simulations investigate the case of a gradient bias force applied in the center of the nano pore. In this study, we are interested in the case of a pulling force at one end of the translocating polymer. Kantor and Kardar were the first to tackle the issue of a translocation driven by a pulling force and predicted $\nu=2$ and $\delta =1$ scaling exponents Appendix A.2. Looking at the translocation time distribution we find that they are in agreement with a first passage probability density function. For a translocation biased by electrophoresis and confirmed for the case of a pulling force [74]. One can estimate the mean translocation velocity which coincides with the average speed deduced from the mean translocation time divided by the chain length. We pushed the analysis further by looking at the average waiting time for the translocation coordinate at different. The translocation coordinate corresponds to the number n of monomers already translocated to the trans side. The average waiting time is the average time that the n th monomer needs to translocate. We find waiting times curves in agreement with the general shape already published in the literature [53] seen in the Fig. 7 In particular, the average waiting time as a function of the translocation coordinate behaves linearly at the beginning of the translocation and for a given pulling force. Thus, at the beginning of the process, the translocation is entirely driven by the pulling force whose influence linearly decreases as it is spread on then monomers already translocated. In this work, we study the linear polymer chain translocation through a nanopore into and out of a spherical cavity with radius R . And here we want to know that the effect of cavity pore size, η , cavity size R and friction coefficient ξ , chain length N and pulling force F for the translocations into cavity and the volume and aspect ratio for out of the cavity, on the translocation processes. The dependence of average translocation time τ , on the geometry and parameter factors, is

presented by with full discussions and with their respective figures.

Results for into the cavity

3.1 Translocation time distribution

The distribution of translocation times for a polymer of chain length $N=16, 48$ and 80 pulled with a force $F=10$ is presented in Fig. 6. The histogram obeys Gaussian distribution. This distribution has a qualitatively different shape compared to that for the free translocation case, where the corresponding distribution is asymmetric, wider and has a long tail [32, 53]. However, this distribution is quite similar to that for driven translocation under an electric field, in that it is narrow without a long tail and symmetric [33, 53]. In all the polymers chain lengths, the stronger the pulling force, the narrower the distribution becomes. As a consequence of this distribution, the average translocation time is well defined and scales in the same manner as the most probable translocation time. Of course, if a weak enough pulling force is used, we still can observe the long tail.

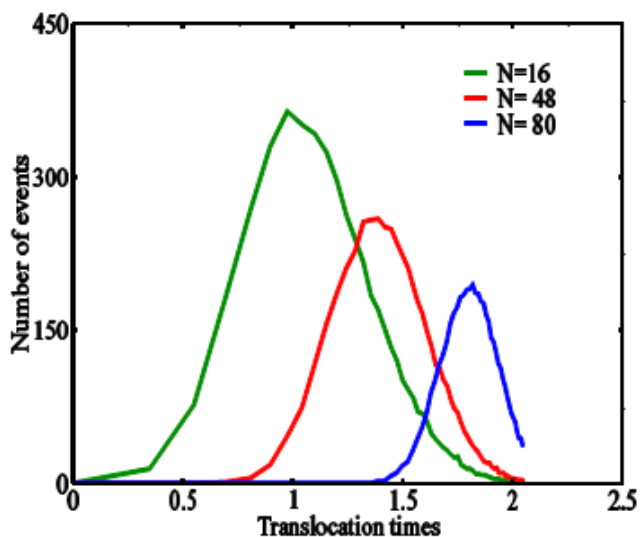


Figure 6. The distribution of 1000 translocation times for a chain of length $N=16, 48$ and 80 under the pulling force of strength $F=10$. Here, the translocation times are normalized by their average value

3.2 Waiting time

We here examine the dynamics of a single segment passing through the pore during translocation is an important issue since the none equilibrium nature of translocation has a considerable effect on it and we moved the analysis further by looking at the average waiting time for the translocation coordinate at $N=16, 48$ and 80 polymerization degrees. The translocation coordinate corresponds to the number n of monomers already translocated to the Trans side. The average waiting time is the average time that the n th monomer needs to translocate (including possible returns if n is not equal to 1 or N). The sum of all the average waiting time over the polymer length gives the average mean translocation time. We find waiting times curves in agreement with the general shape already published in the literature [53] (see Fig. 7). In particular, the average waiting time as a function of the translocation coordinate behaves linearly at the beginning of the translocation and for a given pulling force. Thus, at the beginning of the process, the translocation is entirely driven by the pulling force whose influence linearly decreases as it is spread on the n monomers already translocated. The force is felt only by the trans side and the linear regime is present as long as the diffusion is negligible. When the diffusion force from the cis side compares to the pulling force, a plateau regime is reached. This second regime ends sharply with the retraction of the polymer tail from the cis side. This collapse or retraction of the polymer tail occurs over a constant value but it depends on degrees polymerization

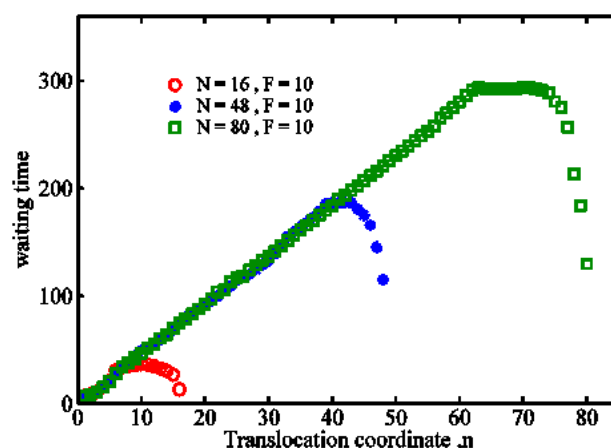


Figure 7. Average waiting time depending on the translocation coordinate at a given force ($F = 10$) for four polymer

3.3 Translocation time as a function of N

For comparison, we here first check out τ as a function of $N = R_g/R$ for two different pore-sizes to this radius R of the spherical cavity, the results shown in Fig8. We obtain in this case that $\tau \sim (R_g/R)^{1.92 \pm 0.01}$ and $\tau \sim (R_g/R)^{2.01 \pm 0.02}$ for pore-size = 1.19 and 1.04 respectively. The value of the pulling force is $F = 10$ and it is in the strong force regime. For this regime, the theoretical prediction is $\tau \sim N^2$ see Appendix A.2. Our numerical result for this pulling force and the pore sizes is in very good agreement with the scaling argument predictions. For a pore of small pore width and a large pore width, the results are shown in Fig. 8. These results are also in excellent agreement with the scaling argument predictions is shown by Appendix A.2 and the scaling arguments for successful translocation provides a useful estimate for the actual translocation through the cavity nanopore size.

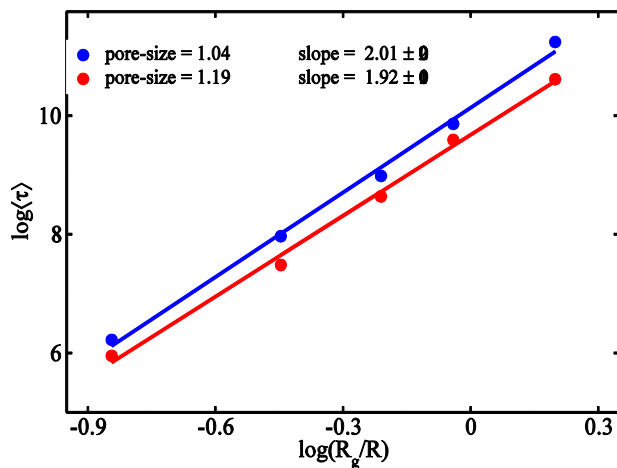


Figure 8 : The translocation time τ as a function of polymer length N which is expressed in terms of the radius of gyration of the polymer, R_g to the radius of the spherical cavity wide pore and a small pore. A constant pulling force of strength $F = 10$ acts on the first monomer.

3.4 Temperature effect on τ

We here examine the other factor, thermostat langevin temperature T influence on the translocation dynamics, Fig.9 shows the translocation time τ as a function of the temperature for pulling force strengths $F = 10$. For the whole, we examined the range of temperatures, τ decreases with increasing temperature for a given pulling force strength of $F = 10$, with this strength increasing temperature τ first rapidly decreases and then approaches saturation at higher temperatures. This temperature dependence of translocation time is in good agreement with experiments [14].

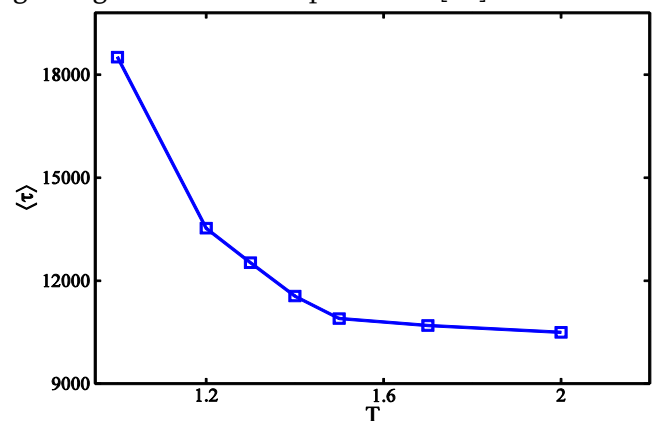


Figure 9. Translocation time as a function of the temperature under the pulling force $F = 10$. The chain length $N = 80$.

3.5 Velocity as function of N

To examine translocation dynamics in detail, we also calculated the translocation velocity v as a function of polymer length N . The translocation velocity can be measured in several ways a simple way is to measure the average horizontal velocity of the center of mass of the polymer over the whole duration of all successful runs Appendix A.1. In Fig.10 we present the polymer velocity as a function of chain length for pulling whose magnitude $F = 10, 13, 16$ and 19 . We get the results for each pulling force which has a good agreement with scaling prediction. There is a clear that the translocation velocity scale as $v \sim (R_g/R)^{-1}$ Appendix A.2 for the regime of strong the pulling force which is in excellent agreement with

the prediction. This simple test confirms that the translocation time takes place because of the translocation velocity.

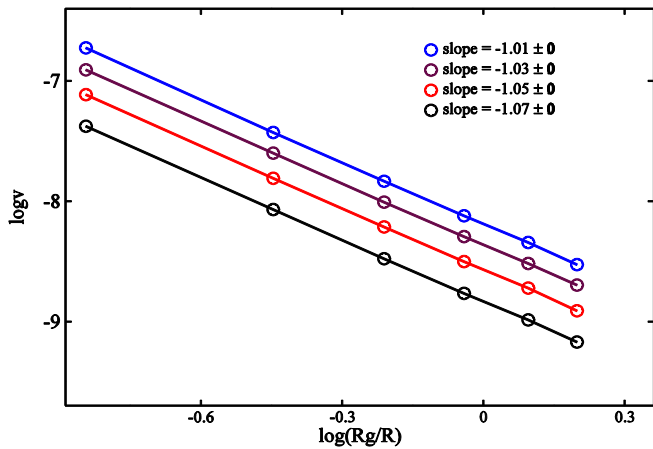


Figure 10. The translocation velocity as a function of polymer length $N = R_g/R$. Data from $F=10, 13, 16$ and 19 are plotted in log-log scale and then the slope is found by a linear fit.

3.6 Force effect on the translocation time

We here examine the other parameter, pulling force F influence on the translocation dynamics by measuring the average translocation time τ . Our theory predicts that there are three regimes in the dependence of the translocation time on the pulling force Appendix A.1. To study this, we again consider first the unimpeded translocation through the widest pore. Thus Fig. 11 confirms that the existence of the three regimes for forces, the value of the pulling force < 0.53 , translocation time is independent of pulling force, this is the weak force regime. With increasing pulling force ,i.e. for $0.53 \leq F < 4.17$ the translocation time scales with the pulling force with an exponent of -0.72 ± 0.03 and for the value of pulling force in the given interval $4.17 \leq F \leq 19$, the exponent is -0.92 ± 0.02 , these are in the limit of moderate and strong force regimes respectively. Finally, it is important to note that both in the case of the external field and pulling force driving the translocation process, there exists a fundamental difference between the Monte Carlo results for the lattice fluctuating bond model and the continuum model considered there in the strong driving force limit. In the Monte Carlo study, the microscopic

transition rate saturates very quickly when the external driving forces increases, leading to a saturation of the velocity and the translocation time [33, 53]. This aspect of the fluctuating bond model is unrealistic and does not correspond to the true dynamics of the system. As seen in the Fig. 12, in the present model we can generalize that the translocation time scales as $\tau \sim F^{-1}$ up to the maximum force value studied and shows no sign of saturation Appendix A.2.

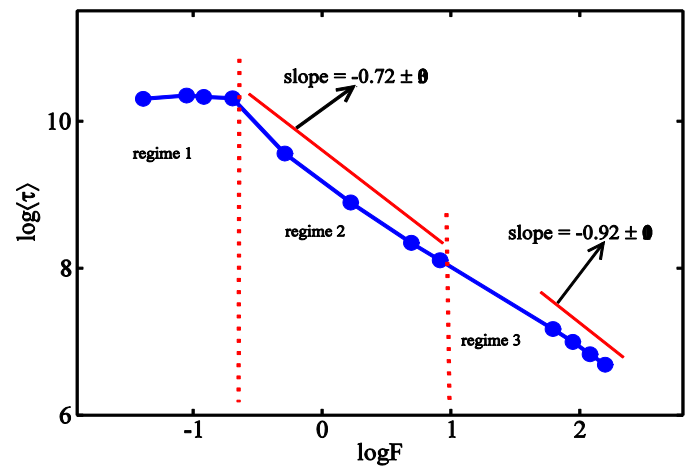


Figure 11. Translocation time as a function of pulling force strength for widest pore an average of 1000 runs. Here, $N = 32$

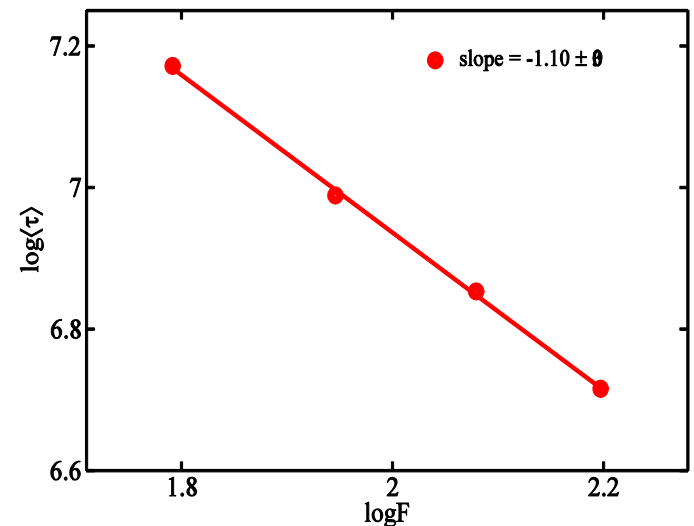


Figure 12 .Translocation time as a function of pulling force strength for small pore τ is an average of 1000 runs. Here, $N = 32$.

Results for Out of the cavity

A. Compression

We here present the discussion for polymer translocation of a 3D spherical cavity with radius R and We examine that net reduction in the variance of the translocation times can be achieved by limiting the maximum extension of the chain's confirmation in the axial direction Fig. 5. Axial compression will clearly reduce the conformational fluctuations along this direction, but it may also decrease the mean translocation time and speeding the translocations processes since the monomers will on average be closer to the pore and it produces more restoring force. We test the impact of compression by simulating the system at a constant radius R while reducing the axial length z_a . The result presented in Fig. 13 shows the mean translocation time $\langle \tau \rangle$ as a function of z_a . Note that since the sphere radius is held constant for each curve (with $R = 11\sigma$, 12σ or 13σ), decreasing z_a corresponds to situations of increased monomer density this is due to change the spherical geometry volume into ellipsoidal geometry volume. As expected, faster translocations arise from decreasing the z_a under such conditions. The highest confinement explored for $R = 13\sigma$ shows a small increase of the translocation time for very short axial ($z_a = 1.5\sigma$) in Fig. 13. Close inspection of these simulations assures that short length scale ordering of the monomers. If we only consider the axial positions of these initial conformations, we note that the monomers are pushed against the two opposite walls and thus create two monolayer stacks Fig. 5.

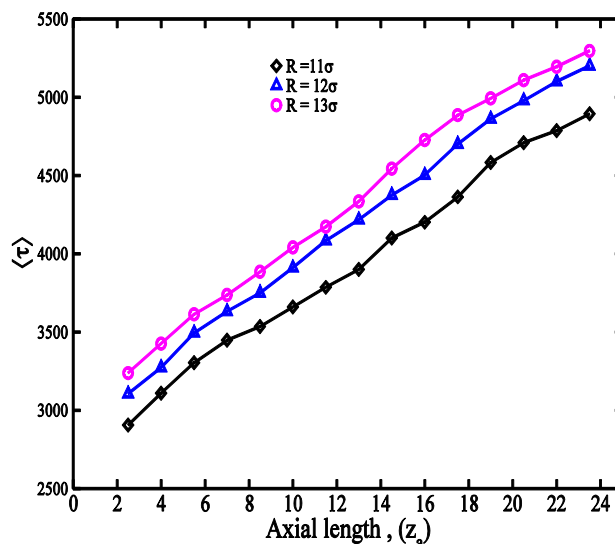


Figure 13. The axial length z_a is varied for three different spherical radius $R = 11\sigma$, 12σ and 13σ . The mean translocation time as a function of z_a .

B. Iso-Volume

In this part simulation results, the confinement volume is held constant and the aspect ratio $a = z_a/2R$. The scaled mean translocation time $\frac{\tau}{\tau^*}$ is plotted as a function of a for four different cavity volumes in Fig. 14. For these volumes, generally, the mean translocation time increases with increasing the volume of the spherical cavity. For fixed volume cavities, the translocation time increases with the aspect ratio. This is because the average monomer distance to the pore increases as the geometry goes from a roughly isotropic three-dimensional cavity to a long axial length. As we discussed previously, bringing the Monomers closer to the pore will lower the translocation time and fast the translocation processes.

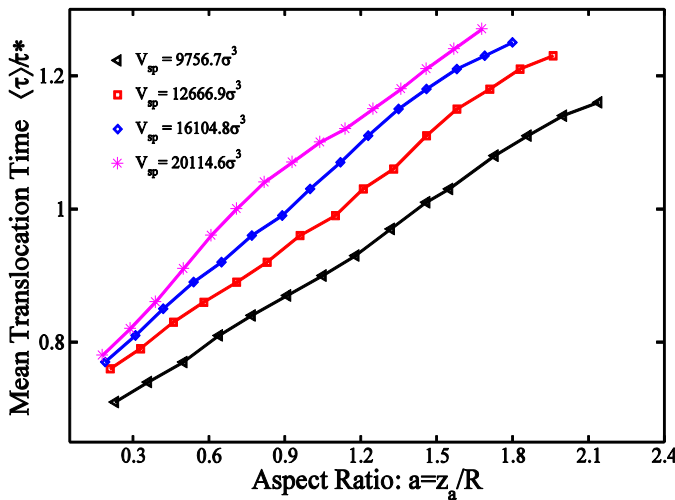


Figure 14. Statistical analysis of the translocation process upon varying the aspect ratio $a = za/2R$ in an ensemble where the volume is kept constant. The mean translocation time as a function of the aspect ratio.

4. Conclusions

We perform a 3D dimensional Langevin dynamics simulation to investigate the translocations of linear polymers under pulling force. There appear clear crossovers on translocation time scaling for linear polymers. We have focused on the influence of the length of the chain length N , the friction coefficient ξ , the temperature T , the cavity nanopore η and the pulling force F on the translocation time. We obtain the distribution of is symmetric and narrow for strong F . $\tau \sim N^2$ and translocation velocity $v \sim N^{-1}$ for both moderate and strong F . Relatively for wide pore, three regimes are observed for τ as a function of F . τ is independent of F for weak F . Finally, the waiting time, for monomer n and monomer $n + 1$ to exit the pore, has a maximum for n close to the end of the chain, in contrast to the case where the polymer is driven by an external force within the pore. We have examined also polymer translocation where the molecule starts inside a finite volume confining spherical cavity. A cavity with a finite axial length can restrict the axial extension of the polymer conformation if it is sufficiently short. When the polymer is initialized in a compressed

state i.e. when the cavity volume is comparable to or less than the equilibrium volume of the polymer conformation mean translocation time is reduced. We measured the mean translocation time for simulations of varying cavity volumes and aspect ratios.

5. Appendix

A. Scaling argument

A.1 stretching extension

The elongation $L(F)$ for a polymer under traction with two forces, F and $-F$, act on its end of the chain may be written as [77].

$$L(F) \sim R\phi\left(\frac{R}{\zeta}\right) \tag{7}$$

Where ϕ is a dimensionless scaling function, $R = N\nu\sigma$, denotes the size of the unperturbed coil, and ζ is the characteristic length of the problem and given by $\zeta = k_B T / F$ For weak forces, such that $F < k_B T / \sigma N^\nu$ the response is linear, i.e. $\zeta(x) \sim x$, which leads to

$$L(F) \sim N^{2\nu} \sigma \left(\frac{F\sigma}{k_B T}\right) \tag{8}$$

For moderate forces regime $k_B T / N^\nu \sigma \leq F \leq k_B T / \sigma$, the chain breaks up into a one-dimensional string of blobs of size ζ .

Then the elongation $L(F) \sim N$, which directs $\zeta(x) \sim x^{(1-\nu)/\nu}$. Thus, one can get

$$L(F) \sim N\sigma \left(\frac{F\sigma}{k_B T}\right)^{\frac{1}{\nu}-1} \tag{9}$$

Finally for strong forces regime $F > k_B T / \sigma$, the chain is nearly fully extended with

$$L(F) \sim N\sigma \tag{10}$$

In the following, we use the same arguments to examine the extension of the tethered chain pulled with a constant force through a viscous medium. The geometrical impediment due to the finite width of the pore is neglected here. For clarity, we assume that the pulling force acts on the last monomer N . Without hydrodynamic interactions the force acting on segment n is given by

$$F_n = \xi \sum_{i=1}^n v_i \quad (11)$$

Where v_i is the velocity of the i^{th} segment. At steady state when inertia can be neglected compared with the frictional force, we assume $v_i = v$ and thus

$$F_n = n\xi v \quad (12)$$

Under this conditions, we stress that the pulling force F equals $F_n = n\xi v$. Here, we encounter a situation in which the tension F_n is segment dependent and where the stretching of the chain is not uniform [53]. To this end, we generalize Eqs.8 and 9 to this situation, following Brochard-Wyart [76], who considered the non uniform deformation of tethered chains in uniform solvent flow. Let $\zeta_n = k_B T / F_n$ is the n -dependent size of the Pincus blobs.

A. Translocation time

To examine τ as a function of N under the same constant pulling force F , we need to know $L(F)$ as a function of the pulling force F , not the drag force ξv on monomer. We need to use relation $F = N\xi v$, which are the same as Eqs. 8 and 9 although the microscopic pictures are different. The polymer travels a distance $L(F)$ during the translocation process. The translocation velocity scales as $N F$ since the force is applied to one monomer only. although the microscopic pictures are different. The polymer travels a distance $L(F)$ during the translocation process. The translocation velocity scales as F/N since the force is applied to one monomer only. Thus the translocation time should depend on N and F as $\tau \sim L(F)/v(F)$ [53]. For moderate forces i.e. $k_B T / N^\nu \sigma \leq F \leq k_B T / \sigma$ we have from the scaling of

$$\tau \sim \frac{L(F)}{v(F)} \sim N^2 F^{-2+\frac{1}{\nu}} \quad (13)$$

This scaling relation for moderate force is the same as the one obtained earlier [53]. We can now extend this approach to both weak and strong forces. For

weak forces, the translocation time scales as

$$\tau \sim \frac{L(F)}{v(F)} \sim N^{1+2\nu} \quad (14)$$

This scaling behavior is the same as that for translocation in the absence of forces. For strong pulling forces, the polymer becomes completely stretched and The translocation time scales as

$$\tau \sim \frac{L(F)}{v(F)} \sim N^{2\nu} F^{-1} \quad (15)$$

Show that $\tau \sim N^2$ for both moderate and strong forces. τ as a function F have three regimes with increasing F see Fig 11

5. Acknowledgments

This work has been supported in part by the International Science Program (ISP), Uppsala University, Sweden , Addis Ababa University (AAU) and Bule Hora University (BHU).

IV. REFERENCES

- [1]. Alberts, B.; Bray, D.; Lewis, J.; Raff, M.; Watson, J.D. Molecular Biology of the Cell; Garland: New York, NY, molecules using a membrane channel. Proc. Natl. Acad. Sci. USA 1996, 93, 13770–13773. USA, 1994; p. 1361.
- [2]. A. Khorshid, P. Zimny, D. T'etreault-La Roche, G. Massarelli, T. Sakaue, and W. Reisner, Phys. Rev. Lett. 113,268104 (2014).
- [3]. SE. Werner, F. Persson, F. Westerlund, J. O. Tegenfeldt, and B. Mehlig, Phys. Rev. E 86, 041802 (2012).
- [4]. L. Dai, J. van der Maarel, and P. S. Doyle, Macromolecules 47, 2445 (2014).
- [5]. A. R. Klotz, L. Duong, M. Mamaev, H. W. de Haan, J. Z. Y. Chen, and W. W. Reisner, acromolecules
- [6]. J. J. Kasianowicz, E. Brandin, D. Branton and D. W. Deaner, Proc. Natl. Acad. Sci. U.S.A. 93, 13770 (1996).

- [7]. L. Gammaitoni, F. Marchesoni, and S. Santucci, *Phys.Rev.Lett.*74,1052(1995).
- [8]. J. J. Kasianowicz, E. Brandin, D. Branton, and D. W. Deamer, *Proc. Natl. Acad. Sci. U.S.A.* 93, 13770 (1996).
- [9]. A. Meller, *J. Phys.: Condens. Matter* 15, R581 (2003).
- [10]. A. Meller, L. Nivon, and D. Branton, *Phys. Rev. Lett.*86, 3435 (2001).
- [11]. A. J. Storm, C. Storm, J. Chen, H. Zandbergen, J.- F. Joanny, and C. Dekker, "Fast DNA translocation through a solid-state nanopore," *Nano Letters*, vol. 5,no.7,pp.1193–1197,2005.
- [12]. W. Sung and P. J. Park, *Phys. Rev. Lett.* 77, 783 (1996)
- [13]. M. Muthukumar, "Polymer translocation through a hole," *The Journal of Chemical Physics*, vol. 111, no.22,pp.10371–10374,(1999).
- [14]. A. Meller, L. Nivon, E. Brandin, J. Golovchenko, and D. Branton, *Proc. Natl. Acad. Sci. U.S.A.* 97,1079 (2000).
- [15]. A. Meller, L. Nivon, and D. Branton, *Phys. Rev. Lett.* 86,3435 (2001).
- [16]. A. Meller and D. Branton, *Electrophoresis* 23, 2583 (2002.)
- [17]. A. J. Storm, C. Storm, J. Chen, H. Zandbergen, J. -F.Joanny and C. Dekker, *Nano Lett.* 5, 1193 (2005)
- [18]. K. Luo, I. Huopaniemi, T. Ala-Nissila, and S.-C. Ying, "Polymer translocation through a nanopore under an applied external field," *Journal of Chemical Physics*, vol. 124, no. 11, Article ID 114704, 2006.
- [19]. I. Huopaniemi, K. Luo, T. Ala-Nissila, and S.-C. Ying, "Langevin dynamics simulations of polymer translocation through nanopores," *The Journal of Chemical Physics*, vol. 125,no. 12,Article ID 124901,2006.
- [20]. C. Forrey and M. Muthukumar, "Langevin dynamics simulations of ds-DNA translocation through synthetic nanopores," *The Journal of Chemical Physics*, vol. 127, no. 1, Article ID 015102,2007.
- [21]. K. Luo, T. Ala-Nissila, S.-C. Ying, and A. Bhattacharya, "Influence of polymer-pore interactions on translocation," *Physical Review Letters*, vol. 99, no. 14,ArticleID148102,2007.
- [22]. K. Luo, T. Ala-Nissila, S.-C. Ying, and A. Bhattacharya, "Heteropolymer translocation through nanopores," *The Journal of Chemical Physics*, vol. 126, no.14, Article ID145101,2007.
- [23]. K. Luo, T. Ala-Nissila, S.-C. Ying, and A. Bhattacharya, "Dynamics of DNA translocation through an attractive nanopore,"*Physical Review E*, vol. 78, no.6,ArticleID061911,2008.
- [24]. M. G. Gauthier and G. W. Slater, "A Monte Carlo algorithm to study polymer translocation through nanopores. II. Scaling laws," *The Journal of Chemical Physics*, vol. 128, no. 20, Article ID 205103,2008.
- [25]. M. G. Gauthier and G. W. Slater, "Sequence effects on the forced translocation of heteropolymers through a small channel," *The Journal of Chemical Physics*, vol. 128, no. 17, Article ID 175103,2008.
- [26]. A. Izmitli, D. C. Schwartz, M. D. Graham, and J. J. De Pablo,"The effect of hydrodynamic interactions on the dynamics of DNA translocation through pores," *The Journal of Chemical Physics*, vol. 128, no. 8, Article ID 085102, 2008.
- [27]. J.-X. Chen, J.-X. Zhu, Y.-Q. Ma, and J.-S. Cao, "Translocation of a forced polymer chain through a crowded channel," *Euro physics Letters*, vol. 106, no. 1, Article ID 18003, 2014.
- [28]. P. Jung and P. Hanggi, *Phys. Rev. A* 44, 8032 (1991a).
- [29]. Z.-H. You, J. Li, X. Gao et al., "Detecting proteinprotein interactions with a novel matrix-based protein sequence representation and support vector machines," *BioMed Research International*, vol. 2015, Article ID 867516, 9 pages, 2015.

- [30]. Z. Yang, S. Li, L. Zhang, A. Ur Rehman, and H. Liang, "Translocation of α -helix chains through a nanopore," *The Journal of Chemical Physics*, vol. 133, no. 15, Article ID 154903, 2010.
- [31]. J. L. A. Dubbeldam, A. Milchev, V. G. Rostiashvili, and T. A. Vilgis, "Polymer translocation through a nanopore: a showcase of anomalous diffusion," *Physical Review E*, vol. 76, no. 1, Article ID 010801, 2007.
- [32]. J. Chuang, Y. Kantor and M. Kardar, *Phys. Rev. E* 65,011802(2002).
- [33]. Y. Kantor and M. Kardar, *Phys. Rev. E* 69, 021806(2004).
- [34]. A. Milchev, K. Binder, and A. Bhattacharya, *J. Chem. Phys.* 121,6042(2004).
- [35]. J. K. F. Luo, T. Ala-Nissila, and S. C. Ying, *J. Chem. Phys.* 124, 034714 (2006).
- [36]. J. K. F. Luo, I. Huopaniemi, T. Ala-Nissila, and S. C. Ying, *J. Chem. Phys.* 124, 114704 (2006)
- [37]. D. Han, P. li, S. An, and P. Shi, "Multi-frequency weak signal detection based on wavelet transform and parameter compensation band-pass multistable stochastic resonance," *Mechanical Systems and Signal Processing*, vol. 70-71, pp. 995–1010, 2016.
- [38]. C. T. A. Wong and M. Muthukumar, "Polymer capture by electro-osmotic flow of oppositely charged nanopores," *The Journal of Chemical Physics*, vol. 126, no. 16, Article ID 164903, 2007.
- [39]. A. Gopinathan and Y. W. Kim, "Polymer translocation in crowded environments," *Physical Review Letters*, vol. 99, no. 22, Article ID 228106, 2007.
- [40]. Milchev, A. Single-polymer dynamics under constraints: Scaling theory and computer experiment. *J. Phys. Condens. Matter* 2011, 23, 1409–1413.
- [41]. Panja, D.; Barkema, G.T.; Kolomeisky, A.B. Through the eye of the needle: Recent advances in understanding biopolymer translocation. *J. Phys. Condens Matter* 2013, 25, 4977–4984.
- [42]. I. Huopaniemi, K. F. Luo, T. Ala-Nissila, and S. C. Ying, *J. Chem. Phys.* 125, 124901 (2006).
- [43]. Palyulin, V.V.; Ala-Nissila, T.; Metzler, R. Polymer translocation: The first two decades and the recent diversification. *Soft Matter* 2014, 10, 9016–9037.
- [44]. K. F. Luo, T. Ala-Nissila, S. C. Ying, and A. Bhattacharya, *J. Chem. Phys.* 126, 145101 (2007).
- [45]. Polson, J.M. Polymer translocation into and out of an ellipsoidal cavity. *J. Chem. Phys.* 2015, 142, 174903
- [46]. Kong, C.Y.; Muthukumar, M. Polymer translocation through a nanopore. II. Excluded volume effect. *J. Chem. Phys.* 2004, 120, 3460–3466.
- [47]. Cacciuto, A.; Luijten, E. Confinement-driven translocation of a flexible polymer. *Phys. Rev. Lett.* 2006, 96, 238104.
- [48]. Ali, I.; Marenduzzo, D.; Yeomans, J. Polymer packaging and ejection in viral capsids: Shape matters. *Phys. Rev. Lett.* 2006, 96, 208102.
- [49]. Sakaue, T.; Yoshinaga, N. Dynamics of polymer decompression: Expansion, unfolding, and ejection. *Phys. Rev. Lett.* 2009, 102, 148302
- [50]. Matsuyama, A.; Yano, M.; Matsuda, A. Packaging/ejection phase transitions of a polymer chain: Theory and Monte Carlo simulation. *J. Chem. Phys.* 2009, 131, 3282–3285.
- [51]. Ali, I.; Marenduzzo, D. Influence of ions on genome packaging and ejection: A molecular dynamics study. *J. Chem. Phys.* 2011, 135, 10122–10127.
- [52]. Yang, S.; Neimark, A.V. Adsorption-driven translocation of polymer chain into nanopore. *J. Chem. Phys.* 2012, 136, 121–125
- [53]. I. Huopaniemi, K. F. Luo, T. Ala-Nissila, and S. C. Ying, *Phys. Rev. E* 75, 061912 (2007).
- [54]. Rasmussen, C.J.; Vishnyakov, A.; Neimark, A.V. Translocation dynamics of freely jointed Lennard-Jones chains into adsorbing pores. *J. Chem. Phys.* 2012, 137, 144903.

- [55]. Ghosal, S. Capstan friction model for DNA ejection from bacteriophages. *Phys. Rev. Lett.* 2012, 109, 6380–6383.
- [56]. T. Ambjornsson and R. Metzler, *Phys. Biol.* 1, 77(2004); T. Ambjornsson, M. A. Lomholt, and R. Metzler, *J. Phys.: Condens. Matter* 17, S3945 (2005); R. H. Ab-dolvahab, E. R. Ejtedadi, R. Metzler, *Phys. Rev. E* 83, 011902(2011).
- [57]. Zhang, K.H.; Luo, K.F. Dynamics of polymer translocation into a circular nanocontainer through a nanopore. *J. Chem. Phys.* 2012, 136, 185103.
- [58]. W. Yu and K. Luo, *J. Am. Chem. Soc.* 133, 13565 (2011).
- [59]. Al Lawati, A.; Ali, I.; Al Barwani, M. Effect of temperature and capsid tail on the packing and ejection of viral DNA. *PLoS ONE* 2013, 8, e52958
- [60]. Polson, J.M.; Hassanabad, M.F.; McCaffrey, A. Simulation study of the polymer translocation free energy barrier. *J. Chem. Phys.* 2013, 138, 244–251.
- [61]. Mahalik, J.; Hildebrandt, B.; Muthukumar, M. Langevin dynamics simulation of DNA ejection from a phage. *J. Biol. Phys.* 2013, 39, 229–245.
- [62]. Linna, R.P.; Moio, J.E.; Suhonen, P.M.; Kaski, K. Dynamics of polymer ejection from capsid. *Phys. Rev. E* 2014, 89, 052702.
- [63]. Cao, Q.; Bachmann, M. Dynamics and limitations of spontaneous polyelectrolyte intrusion into a charged nanocavity. *Phys. Rev. E* 2014, 90, 060601.
- [64]. D. E. Smith, S. J. Tans, S. B. Smith, S. Grimes, D. L. Anderson, C. Bustamante, *Nature (London)* 413, 748 (2001).
- [65]. P. G. de Gennes, *Proc. Natl. Acad. Sci. U.S.A.* 96, 7262(1999).
- [66]. J. Arsuaga, M. Vazquez, P. McGuirk, S. Trigueros, D.W. Sumners, J. Roca, *Proc. Natl. Acad. Sci. U.S.A.* 102, 9165(2005).
- [67]. R. Kapral, *Adv. Chem. Phys.* 140, 89 (2008).
- [68]. I. Ali, D. Marenduzzo, and J. M. Yeomans, *J. Chem. Phys.* 121, 8635 (2004); *Phys. Rev. Lett.* 96, 208102(2006).
- [69]. K. Kremer and G. S. Grest, *J. Chem. Phys.* 92, 5057 (1991).
- [70]. A. Cacciuto, and E. Luijten, *Nano Lett.* 6, 901 (2006).
- [71]. T. Sakaue, and E. Raphaël, *Macromolecules* 39, 2621(2006).
- [72]. C. Micheletti, D. Marenduzzo, and E. Orlandini, *Phys. Rep.* 504, 1(2011).
- [73]. U. F. Keyser, B. N. Koeleman, S. V. Dorp, D. Krapf, R. M. M. Smeets, S. G. Lemay, N. H. Dekker, and C. Dekker, *Nat. Phys.* 2, 473(2006).
- [74]. H. W. de Haan, D. Sean, and G. W. Slater, *Phys. Rev. E* 91, 022601 (2015).
- [75]. J. Sarabadani, B. Ghosh, S. Chaudhury, and T. Ala-Nissila, *Europhys. Lett.* 120, 38004(2017).
- [76]. F. Brochard-Wyart *Europhys. Lett.* 23, 105 (1993); 26, 511(1994); 30, 387(1995).
- [77]. P. Pincus *Macromolecules* 9, 386 (1976)

Cite this article as :

Fikre Jida, "Polymer Translocation through a Nanopore under a Pulling Force - A 3D Langevin Dynamics Simulation Study ", *Gyanshauryam, International Scientific Refereed Research Journal (GISRRJ)*, ISSN : 2582-0095, Volume 2 Issue 6, pp. 34-47, November-December 2019.
 URL : <http://gisrrj.com/GISRRJ19264>